Pseudo-interpenetrating Polymer Networks Based on Tetrafunctional Epoxy Resins and Poly(methyl methacrylate)

Robério Marcos Alcântara,[1] Alfredo Tibúrcio Nunes Pires,[1] Glaucione Gomes de Barros,[2] Laurence A. Belfiore[3]

[1]*Chemistry Department, Federal University of Santa Catarina, 88040-900, Florianópolis, SC, Brazil*
[2]*Chemistry Institute, Brasilia University, 70919-970, Brasília, Brazil*
[3]*Polymer Physics and Engineering Laboratory, Department of Chemical Engineering, Colorado State University, Fort Collins, Colorado 80523*

Received 17 August 2002; accepted 14 November 2002

ABSTRACT: Pseudo-interpenetrating polymer networks (p-IPNs) of an epoxy resin and poly(methyl methacrylate) (PMMA) were synthesized simultaneously. Methyl methacrylate (MMA) was polymerized with benzoyl peroxide in the presence of an oligomeric epoxy resin, which contained stoichiometric amounts of either a tetrafunctional [i.e., ethylenediamine (EDA)] or hexafunctional [i.e., triethylenetetramine (TETA)] crosslinking agent. The resulting materials would be useful for aerospace, automotive, medical, and dental applications. The structure of the epoxy resin (i.e., tetraglycidyl 4,4′-diamine diphenyl methane) was confirmed by elemental analysis and IR and NMR spectroscopies. The thermal, mechanical, and kinetic behaviors of the polymeric networks produced from this oligomeric epoxy resin and the p-IPNs of this crosslinked epoxy with linear PMMA were compared. Time-resolved IR spectroscopy of the cyclic ether group in the epoxy at 906 cm^{-1} revealed kinetic information between 40 and 80°C for a complex reaction scheme. In the absence of MMA, the asymptotic final conversion of epoxide groups was achieved after (1) 60 min of chemical crosslinking at 50°C and (2) 30 min of crosslinking at 80°C with tetrafunctional EDA. In the presence of 10 wt % MMA, asymptotic final conversions of the epoxide group were achieved after (1) 150 min at 40°C, (2) 80 min at 50°C, and (3) 30 min at 80°C. In agreement with other kinetic studies based on the same epoxy resin but different crosslinking agents, these solvent-free polymerizations were diffusion-controlled during the later stages of chemical crosslinking because the apparent reaction order was very close to unity, via an unsteady state batch reactor model with lumped-parameter kinetics. The thermal expansion coefficients of the crosslinked epoxy resin increased at higher concentrations of PMMA, but hexafunctional TETA produced a higher crosslink density and reduced the thermal expansion relative to the same networks and p-IPNs prepared with tetrafunctional EDA. Elastic modulus, fracture stress, and toughness increased synergistically when the epoxy resin was crosslinked with EDA at 40°C in the presence of 10 wt % MMA. This p-IPN exhibited minimal shrinkage, on the order of 0.15%, during the actual polymerization.
 J Appl Polym Sci 89: 1858–1868, 2003

Key words: diffusion; crosslinking; kinetics; thermal properties; mechanical properties

INTRODUCTION

Pseudo-interpenetrating polymers are produced from at least two different components, yielding an intricate network of dissimilar entangled chains. Permanent entanglements occur when one component is crosslinked or synthesized in the presence the other one and physical separation is not allowed.[1–4] This is one of the very few routes for mixing linear polymers and crosslinked polymers on a molecule-for-molecule basis. Although pseudo-interpenetrating polymer networks (p-IPNs) can be classified as immiscible polymer blends,[4] the simultaneous polymerization of one component and crosslinking of the other component promote phase continuity.[5–9] These complex networks might exhibit synergistic thermophysical properties.[7,10,11] Among the various classes of thermosetting polymers, epoxy resins are some of the most important matrices used for high-performance composites, adhesion, lamination, casting, fiber reinforcement, and electronic encapsulation because of their excellent mechanical and thermal properties. However, brittleness, shrinkage, and high levels of moisture absorption represent a few of the physical properties of epoxies that limit their usefulness in general.[12–15] The chemistry of modern dental fillings is based on bulky methacrylate monomers, which polymerize by a free-radical mechanism and contain a significant fraction of finely dispersed ceramics.[16] The thermal and mechanical properties of poly(methyl methacrylate) (PMMA) composites are important because these potential dental

Correspondence to: L. A. Belfiore (belfiore@engr.colostate.edu).

Contract grant sponsor: Brazilian Agency, Coordenação de Aperfeiçoamento de Pessoal de Nível (CAPES).

materials are subject to temperature variations, which might cause them to expand, contract, or experience dimensional distortions during the polymerization process.[17] The primary objectives of this research investigation were to (1) prepare simultaneous p-IPNs from tetraglycidyl 4,4′-diamine diphenyl methane (TGDDM) and methyl methacrylate (MMA), (2) use high-temperature IR spectroscopy to investigate their solvent-free polymerization kinetics, and (3) identify conditions that yielded attractive dental materials based on the considerations of morphology and thermomechanical properties. Similar p-IPNs based on polystyrene with the same epoxy resin, TGDDM, crosslinked with either ethylenediamine (EDA) or triethylenetetramine (TETA), were reported in a previous study.[18] Recently, interpenetrating polymer networks (IPNs) have been developed from poly(amidoamine-organosilicon) copolymeric dendrimers with an EDA core and an organosilicon exterior.[19] The second component is either crosslinked PMMA or cellulose acetobutyrate.[19] These dendrimer-based IPNs form coordination complexes with Cu(II) in methanol.

EXPERIMENTAL

Materials

The epoxy resin TGDDM (Araldite MY720) was supplied by Ciba (Tarrytown, NY) and was used as received. MMA, EDA, TETA, and benzoyl peroxide were purchased from Aldrich Chemical Co. (Milwaukee, WI). All of the reagents were used without further purification.

Chemical characterization of the epoxy resin

Ambient-temperature IR and NMR spectroscopies were used[18] to verify the presence of important functional groups in the epoxy resin, TGDDM. Vibrational absorptions at 1190 and 1512 cm^{-1} were attributed to C═C stretching of the epoxy's aromatic ring. IR signals at 906 and 1250 cm^{-1} corresponded to symmetric and antisymmetric deformations of the epoxide group (i.e., cyclic ether), respectively. High-resolution liquid-state ^{1}H-NMR at 250 MHz identified the presence of epoxide, glycidyl, aromatic, and methylene groups. Elemental analysis of the epoxy resin yielded the following results: 70.3% carbon, 15.8% oxygen, 7.3% hydrogen, and 6.6% nitrogen.[18] These data from elemental analysis suggested the molecular formula $C_{25}H_{30}O_4N_2$ and agreed with predictions based on the chemical structure of TGDDM to within 4% (e.g., 15.8% actual vs. 15.2% predicted for oxygen), possibly because of absorbed moisture.

Synthesis of polymer networks and simultaneous p-IPNs based on the TGDDM epoxy resin

TGDDM was mixed with either EDA or TETA in stoichiometric proportions to prepare crosslinked networks. These mixtures were stirred at ambient temperature and polymerized under a vacuum at temperatures between 40 and 80°C. In a separate flask, p-IPNs were synthesized by the addition of MMA and 2 g of benzoyl peroxide per 100 mL of MMA to the epoxy resin at compositions of 10/90, 20/80, and 30/70 (i.e., MMA/TGDDM w/w), followed by the addition of stoichiometric amounts of either EDA or TETA with respect to TGDDM. These mixtures were stirred at room temperature for 10 min. Then, polymerization and crosslinking occurred for at least 12 h at temperatures between 40 and 80°C.

Physical characterization of networks and p-IPNs

IR spectroscopy

IR spectra were obtained on a Galaxy series model 5020 FTIR from Mattson Instruments (Madison, WI). Samples were deposited on KBr crystals, and spectra were recorded at various times during kinetic studies. A heated transmission cell for solid films from Thermo Nicolet (model HT-32; Madison, WI) provided high-temperature capabilities within the sample chamber for kinetic studies. Temperature control was accomplished via a Eurotherm 818P15 programmable microprocessor (Leesburg, VA) with an accuracy of ±1°C. We generated each spectrum by signal averaging 16 interferograms at a resolution of 1 cm^{-1}, and a triangular apodization smoothing function was used before Fourier transformation. The spectrometer exhibited a signal-to-noise ratio of approximately 300 at ambient temperature, on the basis of four scans at 2-cm^{-1} resolution, with a thin polystyrene film cast from tetrahydrofuran onto a KBr crystal. The signal-to-noise ratio was determined from peak-height measurements on the 1493-cm^{-1} signal of atactic polystyrene, which exhibits a full width at half-height of 6.3 wavenumbers.

Thermogravimetric analysis (TGA)

Thermal degradation measurements were obtained with a Shimadzu TGA-50 thermogravimetric analyzer (Columbia, MD) from 25 to 700°C at a heating rate of 10°C/min. Sample masses were between 8 and 10 mg. The flow rate of the helium purge gas was 50 mL/min.

Dilatometry

Linear coefficients of thermal expansion were obtained with a Shimadzu TMA-50 thermomechanical analyzer from 25 to 140°C at a heating rate of 10°C/

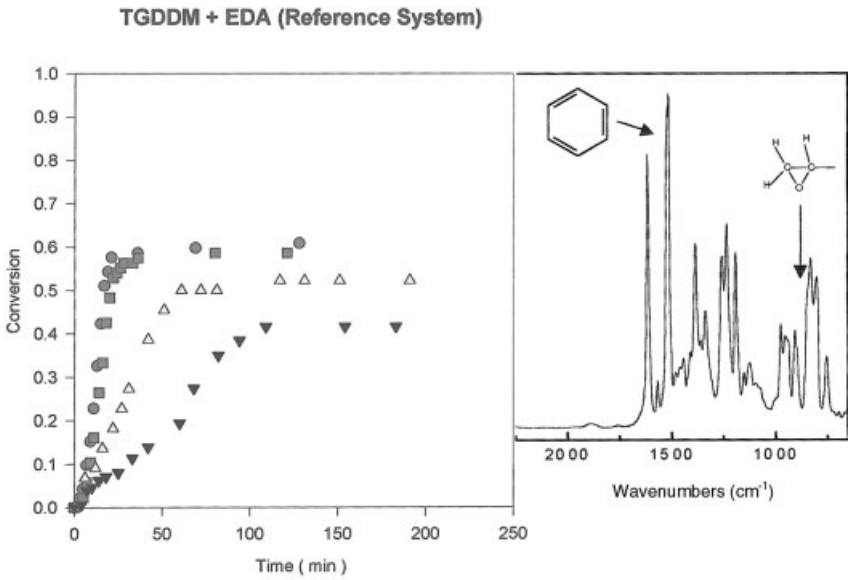

Figure 1 IR-determined time dependence of the fractional conversion of the epoxy groups in TGDDM that reacted with stoichiometric amounts of EDA at the following temperatures: (▼) 40, (△) 50, (■) 70, and (●) 80°C. MMA was not present in these crosslinked networks. The IR spectrum between 700 and 2250 cm^{-1} in the inset illustrates the symmetric deformation of cyclic ether groups at 906 cm^{-1}, which was used to calculate the fractional conversion of the epoxy during chemical crosslinking via eq. (1). The internal reference based on aromatic C═C stretching was identified at 1512 cm^{-1}.

min. Cylindrical samples had an initial diameter of 10 mm and an initial length of 12 mm (i.e., z direction). Free expansion of the sample was measured in the z direction.

Dimensional variations

Dimensional variations (i.e., shrinkage) that developed during crosslinking were measured at ambient temperature using a Zeiss ZMC550CA device with a precision of ± 2 μm. Samples were polymerized under a vacuum for 24 h at 40°C and a pressure of 25 lb of force/$in.^2$ (i.e., 172 kPa) with a specially designed circular aluminum mold. The percentage contraction of the samples was calculated from the difference between the internal circumference of the aluminum mold and the external circumference of the sample. At least four measurements were obtained for each sample composition.

Mechanical properties

Engineering stress–strain measurements on dog-bone-shaped samples were performed at ambient temperature with an Instron model 8501 servohydraulic mechanical testing system (Canton, MA), equipped with pneumatic grips from Lloyd Instruments (Fareham, UK). The strain rate was 2.5 mm/min. A 100-N load cell was used for all stress–strain measurements. Samples were polymerized and molded between two Kapton-coated plates at (1) 40°C for 12 h or (2) 50°C for 24 h. The average sample thickness was 0.21 mm, and the initial length of the ASTM D 638M dog-bone profile was 10 mm, with an initial width between 2.0 and 2.5 mm. At least five samples were tested at each composition. The modulus of elasticity and fracture stress were calculated using the original stress–strain data without smoothing. Toughness was calculated from the area under the stress–strain curve.

Scanning electron microscopy (SEM)

Topological features of the networks and p-IPNs were studied via SEM with a Philips model EX30 at an accelerating voltage of 20 kV. Samples were frozen in liquid nitrogen, fractured, mounted on a stub with silver paint, and coated with an approximate 90-Å layer of gold for 60 s in a Hummer V sputter coater (model SDC 050), operating at 40 mV.

RESULTS AND DISCUSSION

Variable-temperature IR kinetic studies

There are several references to the research literature with the following overlapping keywords: TGDDM, epoxy, networks, and kinetics.[20–33] In this investigation, the symmetric deformation of the cyclic ether group at 906 cm^{-1} was used to monitor chemical crosslinking reactions involving TGDDM, whereas the aromatic C═C stretch at 1512 cm^{-1} in this tetrafunctional epoxy resin served as an internal reference for all of the samples. The IR signal of interest at 906 cm^{-1} and the internal reference at 1512 cm^{-1} are illustrated

in the inset of Figure 1. Significantly better resolution was obtained for the symmetric deformation of cyclic ether groups at 906 cm^{-1} relative to the antisymmetric deformation at 1250 cm^{-1}. Spectra were obtained over a time span of 200 min, and the fraction (α) of epoxy groups that reacted with tetrafunctional EDA was calculated from the net spectral absorbance at 906 cm^{-1} via Beer's law, as follows:

$$\alpha(t) = \frac{[\text{Absorbance } (t=0)]_{906\ cm^{-1}} - [\text{Absorbance } (t)]_{906\ cm^{-1}}}{[\text{Absorbance}(t=0)]_{906\ cm^{-1}}} \quad (1)$$

where t represents polymerization time.

Because the epoxide groups in TGDDM participate in several chemical reactions that constitute the formation of a network,[27–29] α in eq. (1) represents the overall conversion based on all of the possible reactions that involve the cyclic ether. If kinetic rate expressions are formulated in terms of conversion, quantitatively, then one should introduce a different extent of reaction for each independent step in the mechanism so that the molar densities of all of the reactive species can be related to these extents of reaction. In some cases,[34] the conversion of the key limiting reactant is defined such that α approaches 100% if postcure conditions are achieved. On the basis of spectral absorbance at 906 cm^{-1} and eq. (1), the complete conversion of the epoxy did not occur at the reaction temperatures that were investigated in this study. This is consistent with the results of a similar IR investigation of chemical crosslinking and network formation,[20] where nonstoichiometric amounts of TGDDM and *cis*-1,2,3,6-tetrahydrophthalic anhydride required rather high postcuring temperatures to reduce the concentration of excess unreacted epoxide groups. The time dependence of α is illustrated in Figure 1 for stoichiometric proportions of TGDDM and EDA at 40, 50, 70, and 80°C, where the asymptotic final conversion of epoxide groups ranged from 42% at the lowest temperature to 61% at the highest temperature. These IR-determined equilibria or final conversions of the epoxide group in TGDDM crosslinked via EDA (i.e., 42% at 40°C, 52% at 50°C, 59% at 70°C, and 61% at 80°C) were somewhat lower, yet more accurate, than that calculated at 40°C from kinetic measurements using isothermal and dynamic differential scanning calorimetry experiments with the same crosslinking agent (i.e., EDA).[18] Figure 2 illustrates the time dependence of the fractional conversion of epoxide groups for TGDDM, EDA, and 10 wt % MMA at 40, 50, 70, and 80°C, where the temperature-independent equilibrium conversion of epoxide groups was about 55%. The rate of consumption of cyclic ether groups in TGDDM to yield a network structure (1) was approximately independent of the concentration of epoxide groups at low conversion, indicative of zeroth-order kinetics, and (2) increased at a higher temperature on the basis of the slopes of the curves in Figure 1 without MMA, and in Figure 2 with 10 wt % MMA. There are at least three chemical reactions that involve the epoxide group and EDA[34] to yield a polymeric network in the absence of MMA. These reactions are discussed in the next section. Because each step requires an unreacted epoxide group in TGDDM and complete conversion of the cyclic ether does not occur based on long-time IR data at 906 cm^{-1}, the following unsteady state lumped-parameter kinetic model was used to analyze the transient IR results during the later stages of the crosslinking reactions:

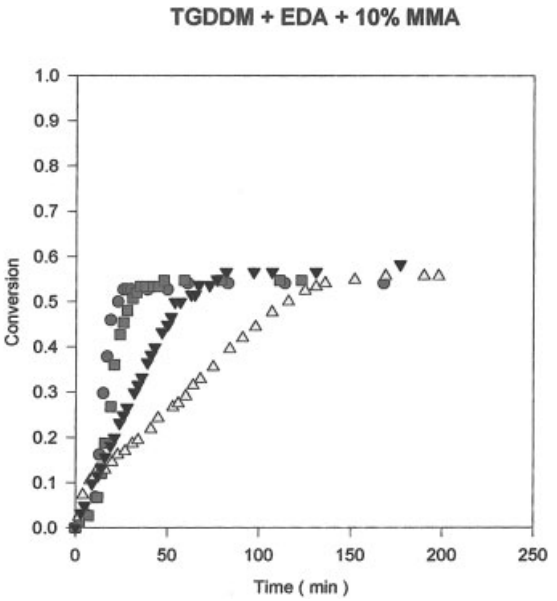

Figure 2 IR-determined time dependence of the fractional conversion of the epoxy groups in TGDDM that reacted with stoichiometric amounts of EDA in the presence of 10 wt % MMA. Isothermal experiments were performed at the following temperatures: (△) 40, (▼) 50, (■) 70, and (●) 80°C.

$$-\frac{dC_{\text{epoxy}}}{dt} = k_n(T)(C_{\text{epoxy}} - C_{\text{equilibrium}})^n \quad (2)$$

where C_{epoxy} is the concentration of epoxide groups at time t, $C_{\text{equilibrium}}$ represents the epoxy concentration at infinite time, n is the apparent order of the overall crosslinking reaction, and $k_n(T)$ is a temperature-dependent nth-order kinetic rate constant with dimensions of (volume/mole)$^{n-1}$/time. Beer's law was used to relate the net spectral absorbance (A) and concentration (C) via the molar absorption coefficient (ε) and path length (δ). Then, the unsteady state kinetic model, given by eq. (2), was re-expressed in terms of the time dependence of the cyclic ether absorbance at 906 cm^{-1}:

TABLE I
Temperature Dependence of IR Kinetic Parameters During the Later Stages of the Crosslinking Reactions for Stoichiometric Amounts of TGDDM and EDA With and Without MMA

Material	Temperature (°C)	n	λ (min)
TGDDM/EDA	50	0.82	1.3×10^2
	70	0.90	8.1×10^1
	80	0.95	6.6×10^1
TGDDM/EDA/10% MMA	50	0.88	1.8×10^2
	70	0.91	1.3×10^2
	80	0.94	1.1×10^2

$$-\frac{d}{dt}A_{906\ \mathrm{cm}^{-1}} = \frac{(A_{906\ \mathrm{cm}^{-1}} - A_{906\ \mathrm{cm}^{-1},\ \mathrm{equilibrium}})^n}{\lambda(T)} \quad (3)$$

where the temperature-dependent characteristic chemical reaction time constant (λ) for nth-order irreversible kinetics is defined by

$$\lambda(T) = \frac{(\varepsilon\delta)^{n-1}}{k_n(T)} \quad (4)$$

We used a similar strategy to analyze transient IR data for TGDDM and EDA in the presence of MMA. Ambient-temperature spectroscopic evidence that the vinyl monomer polymerized to yield PMMA interspersed within the network produced by TGDDM and EDA was obtained from the carbonyl stretching vibration in the ester functional group, whose superficial absorption peak shifted from 1722 cm^{-1} in MMA to 1727 cm^{-1} in PMMA after 3 h under polymerization conditions.[35] There was also a significant decrease in the carbon–carbon double-bond stretching vibration at 1639 cm^{-1} as the vinyl monomer was converted to linear polymer.[35] Because MMA was not the major component in these p-IPNs and the C═C stretch at 1639 cm^{-1} was rather weak and not completely resolved, we evaluated the effect of MMA on the kinetics of network formation by focusing on the cyclic ether deformation at 906 cm^{-1}. Transient analysis of this IR signal in TGDDM was based on a linear least-squares regression of the logarithmic form of eq. (3), which yields a slope of n and an intercept given by $-\ln[\lambda(T)]$. These parameters (n and λ) are summarized in Table I during the later stages of the crosslinking reactions at temperatures between 50 and 80°C for TGDDM and EDA, with and without MMA. For each case summarized in Table I, an apparent reaction order close to unity suggested that these solvent-free polymerizations were diffusion-controlled as networks and p-IPNs were produced with characteristic time constants between 66 and 180 min that (1) decreased at higher temperature and (2) increased when 10 wt % MMA was present. An increase in λ, or a decrease in the apparent kinetic rate constant for the formation of the epoxy network in the presence of MMA, is consistent with a sterically hindered environment due to the mutual entanglement of dissimilar chains.[34] A diffusion-controlled mechanism was used to model crosslinking kinetics during the later stages of the reaction between TGDDM and an aromatic amine crosslinking agent in the presence of bisphenol-A polycarbonate.[21] Furthermore, calorimetric studies of the crosslinking kinetics[22] of TGDDM and 4,4′-diaminodiphenylsulfone in blends with bisphenol-A polycarbonate yielded simple nth-order rate laws with values of n between 1.2 and 1.5.

The multiple reaction scheme presented in the next section reveals that the consumption of cyclic ether groups in TGDDM should have followed second-order kinetics if diffusion were not an intruder during the later stages of these solvent-free polymerizations with either tetrafunctional EDA or hexafunctional TETA. The temperature dependencies of λ and $k_n(T)$ follow an Arrhenius model. As suggested by eq. (4), λ decreases and $k_n(T)$ increases at higher temperatures. Because the empirical reaction order n exhibits weak dependence on temperature, it was not possible to analyze ln k_n versus reciprocal absolute temperature and extract an overall activation energy because the units of k_n depend on the value of n. However, the characteristic time constant for a chemical reaction, given by eq. (4), always has dimensions of time. On the basis of the data in Table I, activation energies between 50 and 80°C were calculated from the slope of ln λ versus $1/T$, multiplied by the gas constant. Rather low apparent activation energies of 5.0 kcal/mol without MMA and 3.4 kcal/mol in the presence of MMA were determined from the lumped-parameter kinetic analysis described previously.

Complex reaction mechanism of network formation

Figure 3 provides a schematic representation of network formation via the chemical crosslinking of TGDDM with either EDA or TETA. A sequence of three elementary steps is outlined in this section to describe the generic formation of a network based on TGDDM and multifunctional amines.[34,36–38] As mentioned previously, analysis based on conversion usually requires a different extent of reaction for each independent step in a multiple-reaction sequence, unless α is defined in terms of all of the reactions that involve the key component . It is not possible to relate the molar density of any other species besides the epoxy to overall conversion α unless that species participates in the same reactions with the same stoichiometric coefficients as the key component. The unsteady-state batch reactor model described below in equations (5) through (10) was formulated in terms of molar densities, not conversion or extents of reaction. The following notation

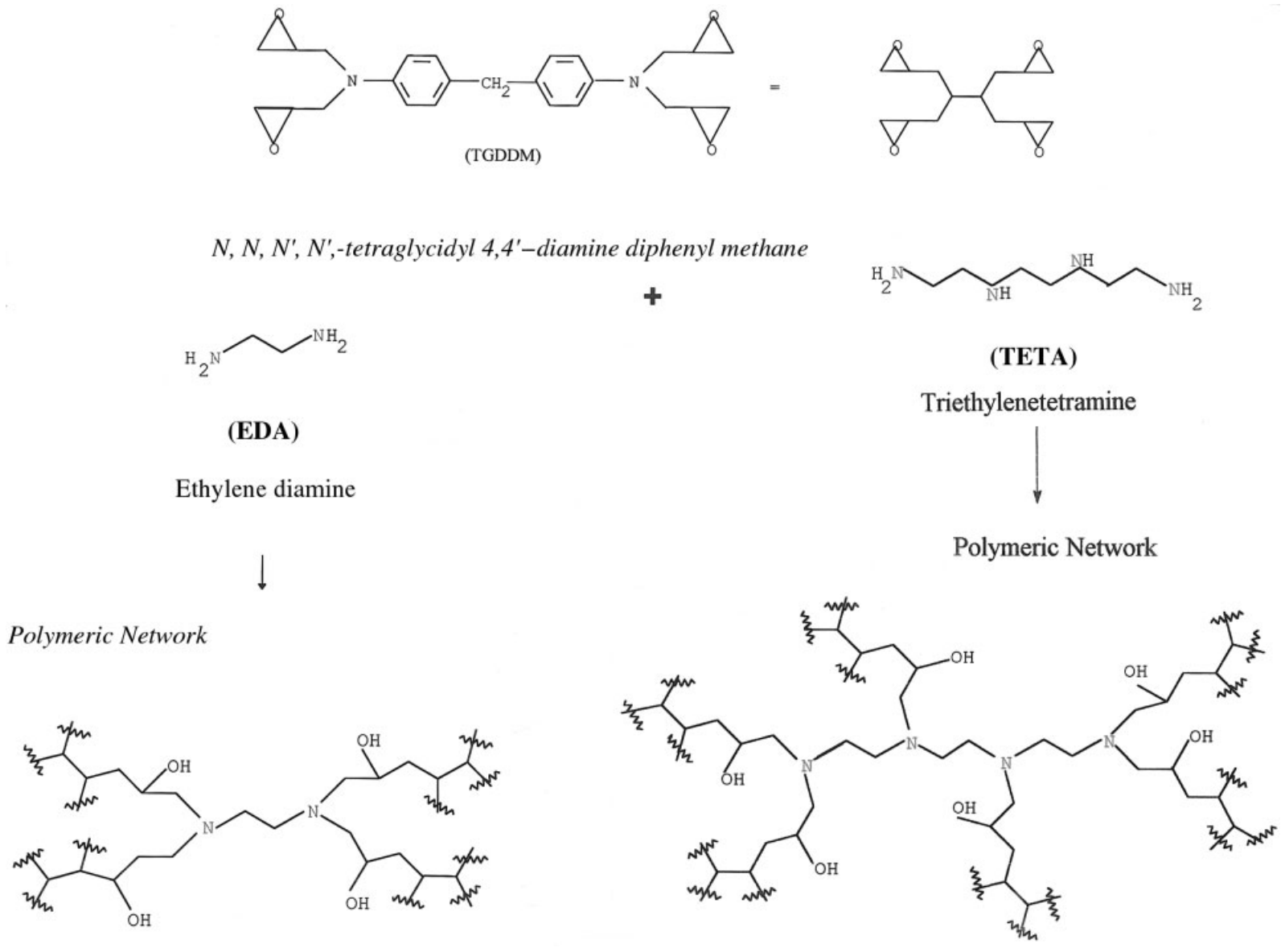

Figure 3 Schematic representations of network formation via the chemical crosslinking of TGDDM with either (left) EDA or (right) TETA in the absence of MMA. The hexafunctional nature of TETA generated a network with a higher crosslink density than that produced by tetrafunctional EDA.

was used to identify the reactive species: TGDDM or epoxy (E), EDA or primary amine (A), secondary amine intermediate (S), network intermediate (N), and polymeric network (P). Initially, cyclic ether groups in the epoxy are cleaved by amino endgroups in EDA to generate a secondary amine intermediate with hydroxyl functionality that catalyzes the second reaction. Schematically, one writes: $E + A \rightarrow S$ for the noncatalytic step, which predominated at low conversion.[36] The kinetic rate law for this bimolecular elementary reaction with the kinetic rate constant k_1 is

$$\text{Rate law}_1 = k_1[E][A] \quad (5)$$

where the brackets indicate molar densities. At a higher conversion of epoxide groups during the later stages of the reaction, cyclic ether groups in TGDDM are cleaved by secondary amine intermediates, which are generated in the first step, to yield more complex network intermediates with hydroxyl functionality, which also catalyze network formation. This catalytic reaction is illustrated schematically as $E + S \rightarrow N$, and it is accelerated by the formation of cyclic hydrogen bonds between the secondary amine, a nearby hydroxyl, and the epoxide group.[34] The kinetic rate law for this bimolecular elementary step with the kinetic rate constant k_2 is

$$\text{Rate law}_2 = k_2[E][S] \quad (6)$$

The presence of hydroxyl functionality in the secondary amine intermediate and the network intermediate (see Fig. 3) catalyzes further reactions of cyclic ether groups in the epoxy with secondary amines that reside in the same molecule as the OH groups, particularly when diffusion-controlled conditions exist during the later stages of the reaction. Primary amines probably do not participate in the following description of network formation because their ability to locate the reaction site is hindered severely by the increased diffusional resistance that accompanies solvent-free polymerizations: $E + S + N \rightarrow P$. The rate law for this catalytic reaction with the kinetic rate constant k_3 is

$$\text{Rate law}_3 = k_3[E][S][N] \quad (7)$$

On the basis of the previous three elementary steps, the rate of consumption of cyclic ether groups in TGDDM is

$$-\frac{d[E]}{dt} = k_1[E][A] + k_2[E][S] + k_3[E][S][N] \quad (8)$$

If the pseudo-steady-state approximation applies to the secondary amine intermediate, then one writes

$$\frac{d[S]}{dt} = \text{Rate law}_1 - \text{Rate law}_2 - \text{Rate law}_3 \approx 0 \quad (9)$$

When the rate laws in eqs. (5)–(7) are combined with eq. (9), one predicts that the rate of consumption of cyclic ether groups via eq. (8) follows second-order chemical kinetics in terms of the molar densities of the epoxy and the amine because

$$-\frac{d[E]}{dt} \approx 2k_1[E][A] \quad (10)$$

where k_1 is the kinetic rate constant for the first reaction, which is not catalyzed by hydroxyl groups. Because stoichiometric amounts of TGDDM and EDA were present initially, the previous result given by eq. (10) could not be classified as a pseudo-first-order process. If additional reactions must be considered[23] or if the crude description of network formation, given by eq. (7), is not an elementary step, then the rate of consumption of cyclic ether groups in TGDDM will differ from the kinetic expression given by eq. (10), but once again, it will not be a first-order process. Hence, variable-temperature IR analysis of the apparent reaction order for TGDDM and EDA during the later stages of chemical crosslinking, with and without MMA, between 50 and 80°C was more consistent with a diffusion-controlled reaction than any of the more complex kinetic rate expressions presented in this section.

TGA

Weight-loss measurements for networks and p-IPNs based on TGDDM, EDA, and MMA are illustrated in Figure 4. Similar behavior was observed for systems that were crosslinked with hexafunctional TETA. There were two separate thermal degradation steps. The liberation of volatile substances was responsible for 2–4% weight loss in the vicinity of 100°C. p-IPNs that contained a higher concentration of PMMA experienced slightly less weight loss in this temperature range. In all of the cases investigated, major weight loss on the order of 75–85% occurred between 350 and 450°C. Once again, there was slightly less weight loss when the p-IPNs contained more PMMA. There did not seem to be much difference in the thermal stability of these p-IPNs when crosslinking was induced by either tetrafunctional EDA or hexafunctional TETA.

Dilatometry

Linear coefficients of thermal expansion between ambient temperature and 140°C are presented in Table II. These coefficients were slightly smaller when the hexafunctional crosslinking agent TETA was used, in

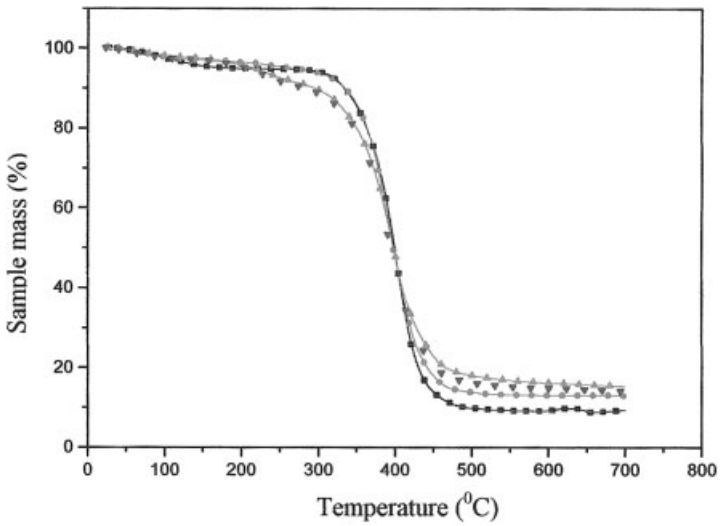

Figure 4 TGA of networks and p-IPNs based on TGDDM, EDA, and MMA, illustrating two different temperature regimes where weight loss occurred. The concentrations of MMA with respect to the epoxy resin were (■) 0, (●) 10, (▲) 20, and (▼) 30 wt %.

comparison to the networks and p-IPNs produced with tetrafunctional EDA. As expected, these results suggested that there was more thermal expansion in networks with lower crosslink density. Schematic representations are provided in Figure 3 to support the claim that EDA produced a lower crosslink density network with TGDDM, relative to TETA. Furthermore, thermal expansion coefficients increased smoothly when the p-IPNs contained more PMMA because linear polymers expand more than crosslinked networks.

Dimensional variations

When subjected to an external pressure of 25 lb of force/in.^{2} (i.e., 172 kPa), networks and p-IPNs contracted slightly during polymerization under a vacuum at 40°C for 24 h. Ambient-temperature measurements of this shrinkage are presented in Table II. When TGDDM was crosslinked with either EDA or TETA, there was very little contraction (~0.15%) at MMA concentrations between 0 and 20 wt %, and there was essentially no effect of the linear polymer (PMMA) on contraction. At 30 wt % MMA in these p-IPNs, there was an approximate three-fold to four-fold increase in the percentage contraction, which was probably caused by polymerization shrinkage of PMMA.[39,40]

TABLE II
Temperature-Average Linear Coefficients of Thermal Expansion between Ambient Temperature and 140°C for Networks and p-IPNs Based on TDGGM, EDA, or TETA, and MMA

Epoxy with crosslinking agent	MMA (wt %)	Thermal expansion coefficient (10^{-4} K^{-1})	Percentage contraction
TGDDM/EDA	0	0.85	0.13
	10	0.90	0.14
	20	1.25	0.18
	30	1.37	0.60
TGDDM/TETA	0	0.75	0.15
	10	0.85	0.13
	20	1.14	0.16
	30	1.23	0.70

Ambient temperature shrinkage was measured for samples that were polymerized under a vacuum at 40°C for 24 h under an external pressure of 25 lb of force/in^2.

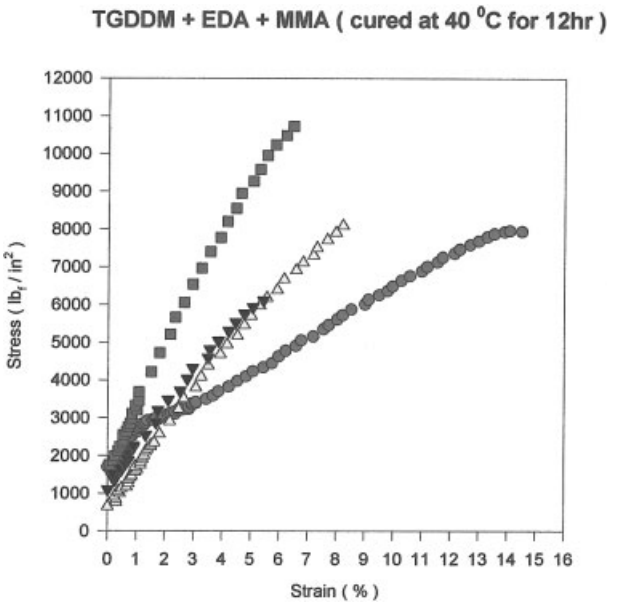

Figure 5 Ambient-temperature engineering stress–strain curves for networks and p-IPNs based on TGDDM, EDA, and MMA. Polymerization occurred under a vacuum at 40°C for 12 h. The strain rate was 2.5 mm/min. The concentrations of MMA with respect to the epoxy resin were (●) 0, (■) 10, (△) 20, and (▼) 30 wt %.

TABLE III
Ambient-Temperature Mechanical Properties of Networks and p-IPNs that Were Polymerized Under a Vacuum at 40° or 50°C

Epoxy with crosslinking agent and temperature	MMA (wt %)	Elastic modulus (10^8 N/m^2)	Fracture stress (10^7 N/m^2)	Toughness (10^6 N/m^2)
TGDDM/EDA	0	7.6	5.7	1.8
40°C	10	11.7	8.2	4.5
40°C	20	8.0	5.3	2.4
40°C	30	7.0	3.9	1.5
TGDDM/TETA	0	7.8	5.4	1.7
40°C	10	9.8	5.7	2.8
40°C	20	8.5	3.5	1.1
40°C	30	6.8	3.0	0.7
TGDDM/EDA	0	8.7	4.1	1.5
50°C	10	10.1	5.8	2.5
50°C	20	8.9	3.5	0.7
50°C	30	5.8	2.9	0.7

Mechanical properties

The ambient-temperature stress–strain response of networks and p-IPNs based on TGDDM, EDA, and MMA is illustrated in Figure 5 for materials that were polymerized at 40°C for 12 h. A summary of the elastic modulus, fracture stress, and toughness of these materials is provided in Table III. For comparison, Table III also contains the corresponding mechanical prop-

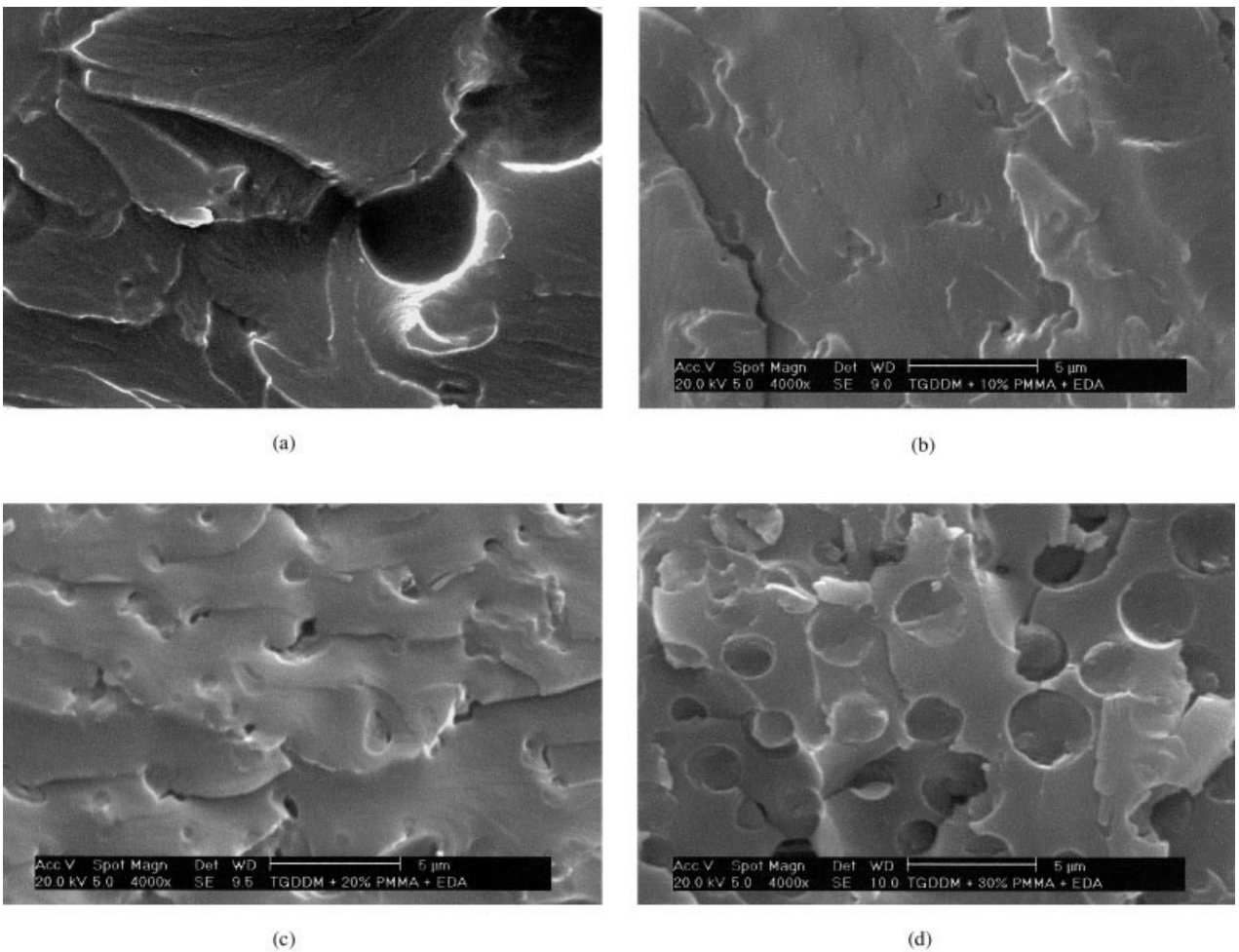

(a) (b) (c) (d)

Figure 6 Scanning electron micrographs of the fracture surface of networks and p-IPNs crosslinked with EDA at a magnification of 4000×. The concentrations of MMA with respect to the epoxy resin (TGDDM) were (a) 0, (b) 10, (c) 20, and (d) 30 wt %.

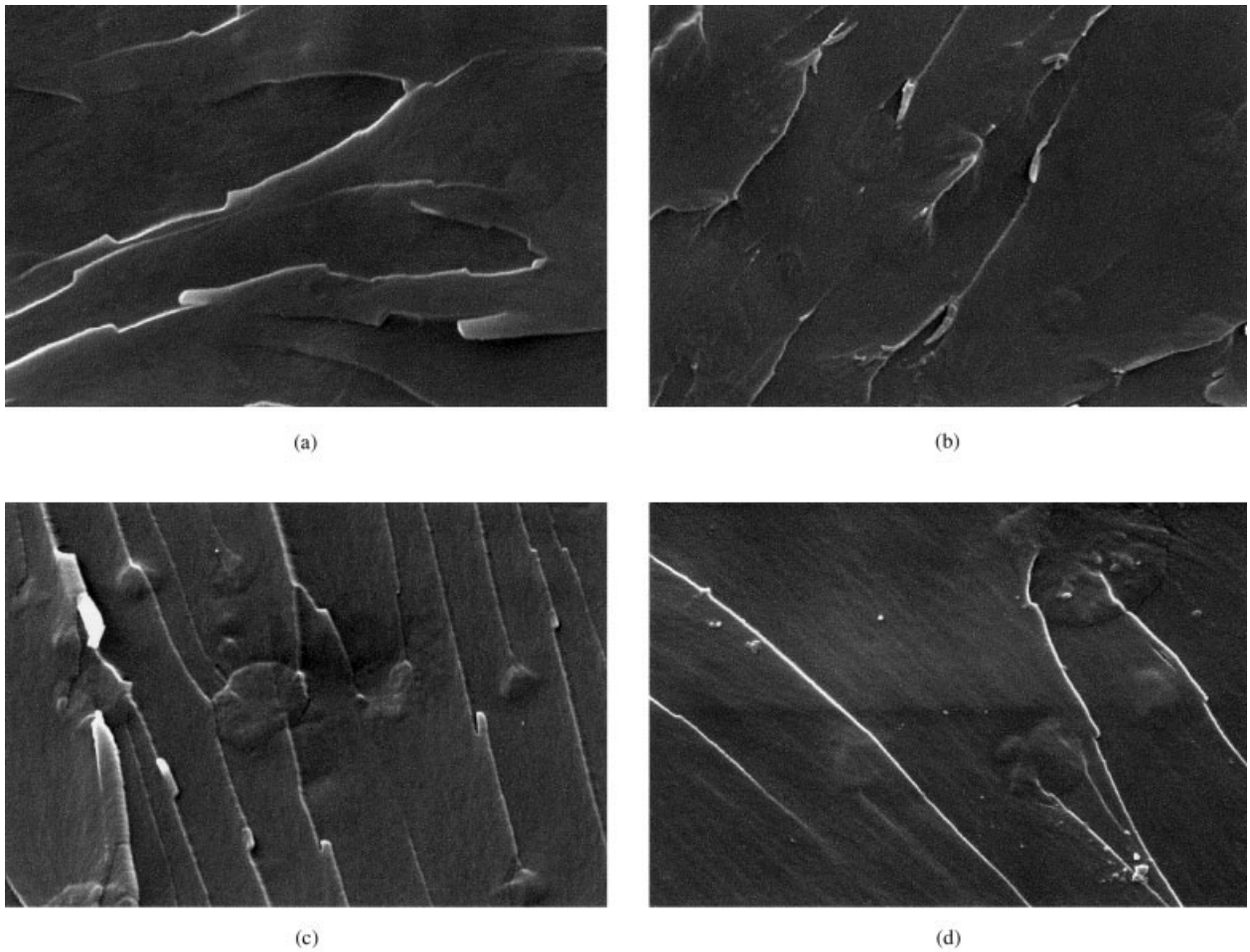

Figure 7 Scanning electron micrographs of the fracture surfaces of networks and p-IPNs crosslinked with TETA at a magnification of 4000×. The concentrations of MMA with respect to the epoxy resin (TGDDM) were (a) 0, (b) 10, (c) 20, and (d) 30 wt % MMA.

erties of similar networks and p-IPNs prepared with (1) TETA at 40°C for 12 h and (2) EDA at 50°C for 24 h. For each type of crosslinking agent and polymerization temperature, the mechanical data in Table III reveal that p-IPNs which contained 10 wt % linear polymer (PMMA) exhibited a synergistic response. Relative to the network produced from TGDDM and EDA at 40°C, the enhancement in elastic modulus (54%), fracture stress (44%), and toughness (150%) was most pronounced when TGDDM was crosslinked with EDA at 40°C in the presence of 10 wt % MMA. When the same system was polymerized at 50°C, the corresponding enhancements in elastic modulus, fracture stress, and toughness were 15, 41, and 67%, respectively, relative to the network produced from TGDDM and EDA at 50°C. When TGDDM was polymerized with the hexafunctional crosslinking agent at 40°C in the presence of 10 wt % MMA, the corresponding enhancements in elastic modulus, fracture stress, and toughness were 26, 6, and 65%, respectively, relative to the network produced from TGDDM and TETA at 40°C. Hence, low concentrations of MMA on the order of 10 wt % with respect to TGDDM were advantageous for developing p-IPNs with attractive mechanical properties and minimal shrinkage.

SEM

Topological features of the fracture surfaces of networks and p-IPNs that were polymerized at 50°C for 24 h are illustrated in Figure 6 for TGDDM/EDA/MMA and in Figure 7 for TGDDM/TETA/MMA. The micrograph of the network produced from TGDDM and tetrafunctional EDA at 4000× magnification revealed a surface that was generally smooth, as illustrated in Figure 6(a). The topology was similar in Figure 6(b), where 10 wt % MMA was introduced into the TGDDM/EDA network. However, cavities appeared in Figure 6(c) at 20 wt % MMA, and the size of these voids increased considerably in Figure 6(d) at 30 wt % MMA. In contrast, all of the SEM micrographs in Figure 7 revealed a smooth laminated topology when the epoxy resin was crosslinked with hexafunctional TETA. These experiments revealed that the presence

of low concentrations of MMA (~10 wt %) did not introduce cavities or voids that might have degraded the mechanical properties of these pseudo-interpenetrating systems that were crosslinked with either EDA or TETA.

CONCLUSIONS

Simultaneous p-IPNs based on TGDDM and PMMA were prepared at temperatures between 40 and 80°C with tetrafunctional EDA or hexafunctional TETA as the crosslinking agent. Ambient-temperature IR spectroscopy identified the presence of PMMA in these p-IPNs via the carbonyl stretch near 1725 cm^{-1}, which shifted to a slightly higher vibrational frequency on polymerization of the vinyl monomer. High-temperature transient IR experiments focused on symmetric deformations of the cyclic ether group in the epoxy resin at 906 cm^{-1} to investigate crosslinking kinetics with and without MMA. A simplified batch reactor model was introduced to analyze lumped-parameter kinetics for a rather complex reaction scheme. Apparent reaction orders close to unity suggested that these solvent-free polymerizations could have been diffusion-controlled during the later stages of chemical crosslinking, but zeroth-order kinetics were more appropriate to describe the consumption of cyclic ether groups at low conversion. The thermal expansion coefficients of these p-IPNs increased at higher concentrations of MMA, but the hexafunctional crosslinking agent TETA caused a reduction in thermal expansion relative to the same networks and p-IPNs crosslinked with tetrafunctional EDA. Neither the crosslinking agent nor the vinyl monomer had much of an effect on shrinkage, which was on the order of 0.15%, when less than 30 wt % MMA is present. Ambient-temperature mechanical properties were enhanced synergistically when p-IPNs crosslinked with either EDA or TETA contained 10 wt % MMA. On the basis of the experiments that were performed, the largest increases in elastic modulus (54%), fracture stress (44%), and toughness (150%) occurred when TGDDM was crosslinked with EDA at 40°C for 12 h in the presence of 10 wt % MMA. In addition to the attractive mechanical response of TGDDM/EDA with 10 wt % MMA for various applications, minimal shrinkage occurred under the actual polymerization conditions at 40°C.

The authors thank Izo Milton Zani, Department of Stomatology, Federal University of Santa Catarina, for the encouragement and motivation to complete this study

References

1. Frisch, H. L.; Frisch, K. C.; Klempner, D. Pure Appl Chem 1981, 53, 1557.
2. Cassidy, E. F.; Xiao, H. X.; Frisch, K. C.; Frisch, H. L. J Polym Sci 1984, 22, 2667.
3. Mishra, V.; Sperling, L. H. J Polym Sci Part B: Polym Phys 1996, 34, 883.
4. Sperling, L. H. Introduction to Physical Polymer Science, 3rd ed.; Wiley-Interscience: New York, 2001; p 143.
5. Das, B.; Chakaborty, D.; Hajra, A. K.; Sinha, S. J Appl Polym Sci 1994, 53, 1491.
6. Das, B.; Chakaborty, D.; Hajra, A. K. Eur Polym J 1994, 11, 1269.
7. Lee, M. C.; Ho, T. H.; Wang, C. S. J Appl Polym Sci 1996, 62, 217.
8. Udagawa, A.; Sakurai, F.; Takahaski, T. J Appl Polym Sci 1991, 42, 1861.
9. Shimbo, M.; Ochio, M.; Shigeta, Y. J Appl Polym Sci 1981, 26, 2265.
10. Tan, S. S.; Zhang, D. H.; Zou, E. L. Polym Networks Blends 1996, 6, 91.
11. Tan, S.; Zhang, D.; Zou, E. Polym Int 1997, 42, 90.
12. Tanaka, N.; Lijima, T.; Fukuda, W.; Tomoi, M. Polym Int 1997, 42, 95.
13. Ying, L.; Mao, J. J Appl Polym Sci 1996, 61, 2059.
14. Lu, S. P.; Xiao, H. X.; Frisch, K. C. Polym Adv Technol 1996, 7, 323.
15. Baidak, A. A.; LiéGeois, J. M.; Sperling, L. H. J Polym Sci Part B: Polym Phys 1997, 35, 1973.
16. Nicholson, J. W.; Anstice, H. M. J Chem Educ 1999, 76, 1497.
17. Usanmaz, A.; Turker, F.; Dogan, A.; Akkas, N. J Appl Polym Sci 1998, 69, 1409.
18. Alcântara, R. M.; Pires, A. T. N.; Belfiore, L. A.; de Barros, G. G. J Polym Eng 2001, 21, 319.
19. Vidal, F.; Hémonic, I.; Teyssié, D.; Boileau, S.; Reeves, S. D.; Dvornic, P. R.; Owen, M. J. Polym Prepr 2001, 42, 128.
20. Guerrero, P.; DelaCaba, K.; Valea, A.; Corcuera, M. A.; Mondragon, I. Polymer 1996, 37, 2195.
21. Su, C. C.; Woo, E. M. J Polym Sci Part B: Polym Phys 1997, 35, 2141.
22. Su, C. C.; Kuo, J. F.; Woo, E. M. J Polym Sci Part B: Polym Phys 1995, 33, 2235.
23. Hseih, H. K.; Su, C. C.; Woo, E. M. Polymer 1998, 39, 2175.
24. Pyun, E.; Sung, C. S. P. Macromolecules 1991, 24, 855.
25. Matejka, L.; Dusek, K. Polymer 1991, 32, 3195.
26. Johncock, P.; Cunliffe, A. V. Polymer 1992, 33, 2392.
27. St. John, N. A.; George, G. A. Polymer 1992, 33, 2679.
28. Debakker, C. J.; George, G. A.; St. John, N. A.; Fredericks, P. M. Spectrochim Acta A, Molecular and Biomolecular Spectroscopy 1993, 49, 739.
29. St. John, N. A.; George, G. A. Prog Polym Sci 1994, 19, 755.
30. Levchik, S. V.; Camino, G.; Luda, M. P.; Costa, L.; Costes, B.; Henry, Y.; Muller, G.; Morel, E. Polym Degrad Stab 1995, 48, 359.
31. Siddarmaiah; Jagadeesh, K. S. J Polym Mater 1996, 13, 223.
32. Corcuera, M. A.; Mondragon, I.; Riccardi, C. C.; Williams, R. J. J. J Appl Polym Sci 1997, 64, 157.
33. Dispenza, C.; Carter, J. T.; Mcgrail, P. T.; Spadaro, G. Polym Eng Sci 2001, 41, 1486.
34. Lin, M. S.; Jeng, K. T.; Huang, K. Y.; Shih, Y. F. J Polym Sci Part A: Polym Chem 1993, 31, 3317.
35. Kaczmarczyk, B.; Morejko-Buz, B.; Stolarzewicz, A. Fresenius J Anal Chem 2001, 370, 899.
36. King, J. J.; Bell, J. P. In Epoxy Resin Chemistry; Bauer, R. S., Ed.; ACS Symposium Series 114; American Chemical Society: Washington, DC, 1979; p 223.
37. Mijovic, J.; Kim, J.; Slaby, J. J Appl Polym Sci 1984, 29, 1449.
38. Moroni, O. A.; Mijovic, J.; Pearce, E. M.; Foun, C. C. J Appl Polym Sci 1986, 32, 3761.
39. Kroschwitz, J. I. Concise Encyclopedia of Polymer Science and Engineering; Wiley: New York, 1990.
40. Klempner, D.; Sperling, L. H.; Utracki, L. A. Interpenetrating Polymer Networks; Advances in Chemistry Series 239; American Chemical Society: Washington DC, 1994.